THE DUCTILE FRACTURE TOUGHNESS OF AN AUSTENITIC-FERRITIC STAINLESS STEEL

R. Roberti* and D. Firrao**

*Dipartimento di Chimica-Fisica Applicata, Politecnico di Milano, Milan, Italy
**Dipartimento di Scienza dei Materiali, Politecnico di Torino, Italy

ABSTRACT

The fracture toughness of an austenitic-ferritic stainless steel has been investigated; J-resistance curves have been obtained by the multiple specimen technique for the steel solution annealed at three different temperatures. Despite the increase of the ferrite content at increasing solution anneal temperature, the fracture toughness remains almost constant.
The relationship between fracture toughness and the microstructural parameters has been investigated in order to interpret the constancy of the fracture toughness and to assess the validity of a model recently proposed by the Authors for the ductile fracture.

KEYWORDS

Ductile fracture toughness, J-integral, duplex stainless steel, ductile fracture models, J-resistance curves.

INTRODUCTION

Two-phase stainless steels with an austenitic-ferritic structure possess a number of interesting properties and their use has been constantly increasing during the last years, in particular in those applications where stress corrosion cracking does not allow the use of the austenitic stainless steels. Their chemical composition, and in particular the percentage of chromium, nickel and molybdenum, is generally adjusted in order to obtain well defined ratios between the microstructural phases austenite and ferrite. When the amount of the ferrite is increased both by chemical composition adjustment or by increasing the solution annealing temperature, these steels have a higher tendency to embrittlement; however, in the standard solution anneal condition these steels have a high toughness and a toughness transition temperature in the range -150 ÷ -50°C, depending on grain size (Peckner and Bernstein (1977).
A research programme has been undertaken in order to characterize the fracture initiation and propagation properties of these steels and to investigate

the relationship between the fracture toughness and the various possible changes of the microstructural parametrs. The results of a first part of this research work are presented here and treat the relationship between the microstructural parameters of an austenitic-ferritic stainless steel solution annealed at increasing temperatures and its room temperature ductile fracture toughness.

EXPERIMENTAL PROCEDURE

The chemical composition of the steel was: C=0.020, Si=1.48, Mn=1.65, P=0.022, S=0.005, Cr=18.70, Ni=4.97, Mo=2.65, N=0.076. The steel had been supplied in the form of a 10 mm thick plate. The solution anneal was performed at three different temperatures: 1050, 1175 and 1300°C, in salt baths for 1 h and subsequent water quench. On increasing the solution anneal temperature, as reported by Nicodemi et al. (1973), in the austenitic-ferritic stainless steels two phenomena can be observed at microstructural level, namely an increase of the amount of the ferrite phase and of the size of the ferrite islands.
All the test specimens were machined in the transverse direction; the standard three point bending specimens for the fracture toughness tests had the plate thickness. In the case of the 1050°C solution anneal treatment some specimens with a width of 10 mm were also utilized. All the fracture toughness specimens were fatigue precracked to a final crack length to width ratio a/W in the range 0.5÷0.6; in all the specimens the fatigue precrack had the TL orientation. Since the steel under investigation exhibits a high room temperature ductility, the fracture initiation and propagation properties are best discussed in terms of an elastic-plastic parameter and in this study the J-integral was used, according to the multiple specimen technique reported in the ASTM E813-81 standard.
The tension and fracture tests were performed at room temperature on a screw-driven, 100kN capacity, INSTRON 1195 machine, at a crosshead displacement rate of 0.083 m/s.
The crack extension Δa in the unloaded specimens was made evident by subsequent fatigue cracking of the remaining ligament; this procedure was preferred instead of breaking apart the specimen at low temperature in order to avoid any deformation of the crack front. Since crack extension was easily distinguishable from the fatigue crack, heat tinting was not applied. The Δa values were obtained as the mean value of nine measurements evenly spaced along the crack front.
Fracture surface examinations were performed by means of a Super ISI III A scanning electron microscope.

RESULTS AND DISCUSSION

The mechanical properties for the three solution anneal temperatures are listed in Table 1, along with the volume fraction of the ferrite phase and the mean interparticle spacing between the non metallic inclusions. It is evident that, despite the increasing of the volume fraction of the ferrite, the room mechanical properties are not modified; at the same time, the inclusion mean spacing and the strain hardening exponent N are not affected by the increase of the solution anneal temperature.
J-resistance curves, drawn according to the ASTM standard, are reported in

Fig. 1; from the figure it can be seen that the experimental data seem to be better described by a power law fit, as alrady reported by other Authors (Voss and Blauel, 1982; Blauel and Schwalbe, 1982; Wilson, 1979); furthermore, the experimental points in correspondence of the blunting line are relative to crack advancement values well higher than those due only to the blunting of the crack tip.
Therefore the blunting line does not seem to be appropriately described by the equation reported in the ASTM standard; this fact has already been pointed out in the literature (Mills, 1981; O'Vrien and Ferguson, 1982; Keller and Munz, 1977), and for high toughness materials it has also been propo-

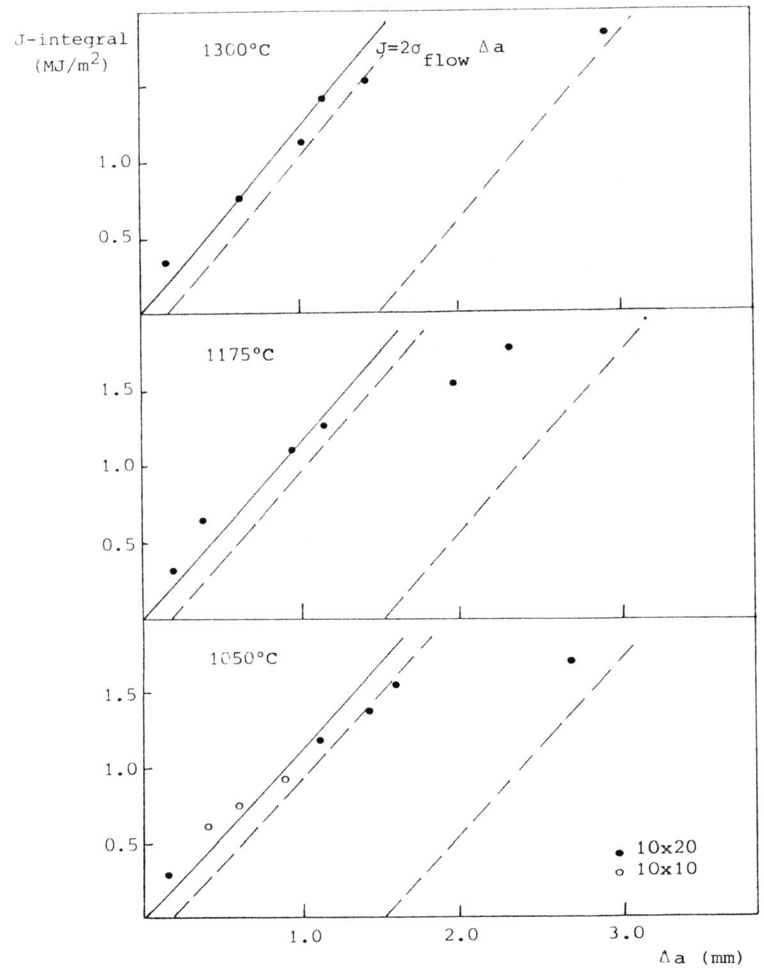

Fig. 1 - J - Δa plots for the austenitic-ferritic stainless steel solution annealed at different temperatures

sed to use a steeper blunting line or to determine it experimentally.
In the present research work a different methodology has been adopted. In fact, as shown in Fig. 2, the streched zone at the crack tip is clearly visible; therefore, in order to avoid the need to use a blunting line difficult to define, the crack advancement has been measured from the end of the stretched zone; such a crack advancement, as it is not affected by the blunting of the crack tip, has been referred to as Δa_{true}. As a consequence the onset of the crack advancement is in correspondence of $\Delta a_{true}=0$ and therefore the critical value of the J-integral must be individuated by back extrapolating the data points to the ordinate axis.

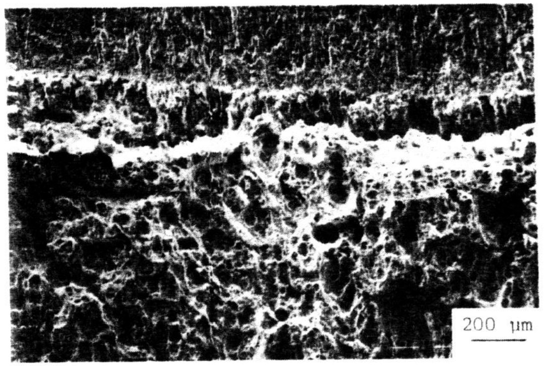

Fig. 2 - Microfractographic aspect of a fracture toughness sample in correspondence of the fracture initiation from the fatigue precrack. 1050°C solution anneal treatment.

Furthermore, as the crack advancement was affected by a pronounced crack tip tunneling, it was decided to measure only the maximum of the Δa_{true}, corresponding to the midsection of the sample; this choice was done also on the basis of some results reported by Kaiser and Hagedorn (1982), from which it can be deduced that the use of the mean or the maximum values of the crack advancement gives the same extrapolated fracture toughness value at the onset of crack propagation.
With the above reported methodologies the plot in Fig. 3 was obtained, where it can be seen that the experimental points are now fitted by linear regres-

TABLE 1 - Mechanical properties and microstructural characteristics of the investigated austenitic-ferritic stainless steel

	σ_{UTS}	σ_Y	Elong.	Reduction of area	N	Impact energy	Ferrite	Inclusion mean spacing
	MN/m^2	MN/m^2	%	%		J	%	um
1050°C	724	452	53	70	0.39	187	54	109-119
1175°C	713	474	46	68	0.39	178	70	109-119
1300°C	726	469	51	68	0.37	188	79	109-119

sion lines with high correlation coefficients.
The critical J-integral values are nearly the same for the three heat treatments and seem to be slightly decreasing at increasing the solution annealing temperature.
It is to be underlined that the specimen thickness and ligament sizes do not meet the ASTM standard restrictions, and therefore the critical J-integral values cannot be considered valid plane strain J_{Ic}; however, it is also to be remembered that in the case of high toughness and high strain hardening steels, such as the austenitic stainless steels, it has been proved that

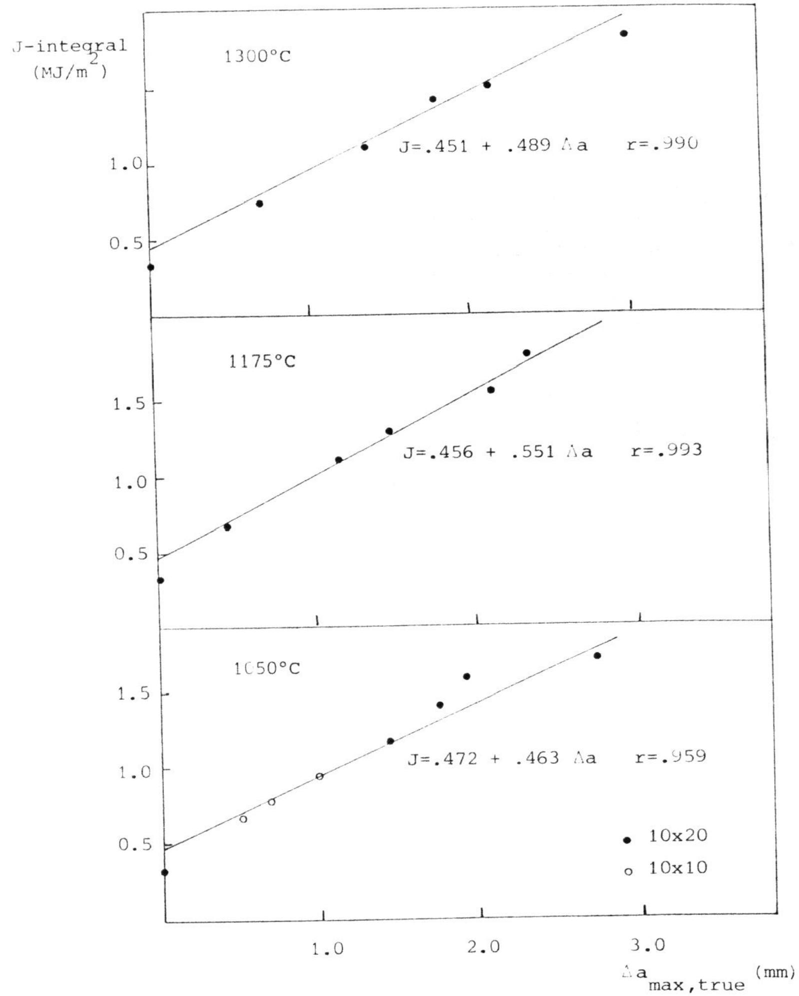

Fig. 3 - J-integral vs. the maximum value of crack advancement, measured from the end of the stretched zone

such restrictions are too restictive (Bumford and Bush, 1979; Nyilas and Krauth, 1982).

As concerns the fact that the steel has almost the same fracture toughness properties despite the different heat treatment conditions, it has to be related to the microfractographic features.

First of all, as reported in Figs. 4 a,c,e showing a section perpendicular to the fracture plane, it can be observed that the fracture doesn't follow a preferential path at the austenite-ferrite interface or within one of these microstructural constituents. Furthermore, the fracture surfaces (Figs. 4 b,d, f) always show a ductile feature, with the typical microdimples at the larger non metallic inclusions.

Therefore, as the different solution annealing heat treatments did not alter both the content and the distribution of non metallic inclusions, it seems to be justified that the fracture toughness has nearly the same value.

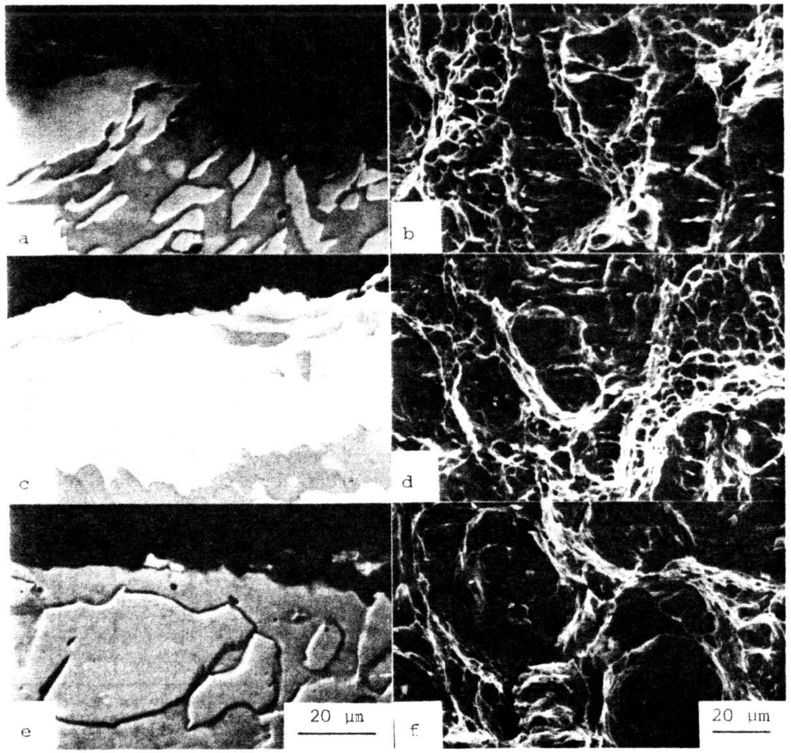

Fig. 4 - Metallographic aspect of a section perpendicular to the fracture plane and microfractographic aspect of fracture surfaces of fracture toughness samples of austenitic-ferritic stainless steel solution annealed at: 1050°C (a,b), 1175°C (c,d), and 1300°C (e,f).

In the case of ductile fracture the Authors have recently proposed a model to relate the fracture toughness to the microstructural parameters (Firrao and Roberti, 1982), and a relationship for J_{Ic} has been obtained as follows:

$$J_{Ic} = \sigma_Y \frac{\varepsilon_{max,f}^{(N+1)}}{F(\Gamma(N))\,\varepsilon_Y^{N}} \rho_{eff}$$

where σ_Y and ε_Y are the yield strength and the yield strain, N the strain hardening coefficient, $\varepsilon_{max,f}$ the maximum strain attainable at the blunted crack tip before fracture nucleation, ρ_{eff} the maximum root radius of the blunted crack tip and $F(\Gamma(N))$ a function of the Γ mathematical function.

The relationship between the microstructural parameters and the ductile fracture toughness is given by the dependence of the terms in the formula on the microstructural parameters. The strain hardening exponent and the yield strength depend on the mean interparticle spacing between the non metallic inclusions; this mean interparticle spacing can be substituted to ρ_{eff}, as it is related to the process zone size at the crack tip, and $\varepsilon_{max,f}$ is an inverse function of the non metallic inclusion volume fraction (Firrao and Roberti, 1983a).

As regards the assessment of the above reported formula, whose applicability has already been proved in the case of different steels (Firrao and Roberti, 1982, 1983b), in Table 2 there are reported the values of the various terms with the calculated values of J_{Ic}. The $\varepsilon_{max,f}$ value in Table 2 has been taken equal to the true fracture strain in monoaxial tension test, as also in such a test, in the region where fracture initiates, a triaxial state of stress is approached, as in plane strain bending tests.

The comparison between the calculated and the experimental values of J_{Ic} demonstrates a good agreement, thus confirming the validity of the proposed formula in relating the ductile fracture toughness to the microstructural parameters.

TABLE 2 - Parameters for the calculation of J_{Ic}

	ε_Y	$\varepsilon_{max,f}$	$F(\Gamma(N))$	J_{Ic} calculated MJ/m^2	J_{Ic} experimental MJ/m^2
1050°C	0.0043	1.024	1.1511	.464 - .506	.472
1175°C	0.0044	1.139	1.1511	.446 - .487	.456
1300°C	0.0044	1.139	1.1292	.402 - .440	.451

CONCLUSIONS

Room temperature fracture toughness tests have been carried out on an austenitic-ferritic stainless steel, solution annealed at different temperatures; despite the increase of the amount of the ferrite phase from 54% to 79%, the fracture toughness remains nearly the same.

The constancy of the fracture toughness has been related to the fact that the increase of the solution anneal temperature does not modify the microstructural parameters that play a role in controlling the fracture mechanism of microvoid nucleation and coalescence.

Finally it has been confirmed the validity of the relationship proposed by the Authors between the fracture toughne*s and the microstructural parameters in the case of ductile fracture.

REFERENCES

Bamford, W.H., and A.J. Bush (1979). Elastic-Plastic Fracture, ASTM STP 668, 553-577.

Blauel, J.G., and K.H. Schwalbe (1982). European Group of Fracture, Task Group 1, Elastic-Plastic Fracture Mechanics, Minutes of the Meeting Held on Sept. 21st, Leoben. Appendix 3.

Firrao, D., and R. Roberti (1982). Strength of Metals and Alloys, Ed. R.C. Gifkins, Pergamon Press, London, 947-952.

Firrao, D., and R. Roberti (1983a). La Metall. Ital., LXXV, 645-651.

Firrao, D., and R. Roberti (1983b). Met. Science and Techn., 1, 5-13.

Kaiser, H.J., and K.E. Hagedorn (1982). Fracture Toughness and the Role of Microstructure, EMAS, London, 76-83.

Keller, H.P., and D. Munz (1977). Flaw Growth and Fracture, ASTM STP 631,217-231.

Mills, W.J. (1981). J. Test. Eval., 9, 56-62.

Nicodemi, W., M. Balbi, and G. Silva (1973). Ist. Lombardo Rend. Scient., A 107, 333-342.

Nyilas, A., and H. Krauth (1982). Fracture Toughness and the Role of Microstructure, EMAS, London, 523-530.

O'Vrien, D.M., and W.G. Ferguson (1982). Int. J. Fracture, 20, R39-R43.

Peckner, D, and I.M. Bernstein (1977). Handbook of Stainless Steels. MacGraw-Hill, New York, 8-10.

Voss. B, and J.G. Blauel (1982). Fracture Toughness and the Role of Microstructure, EMAS, London, 47-56.

Wilson, A.D. (1979). Elastic-Plastic Fracture, ASTM STP 668, 469-492.